Probing the local structure of liquid binary mixtures by x-ray absorption spectroscopy

Angela Trapananti[1,*] and Andrea Di Cicco[1,2]
[1]*Istituto Nazionale per la Fisica della Materia (INFM) and Dipartimento di Fisica, Università degli Studi di Camerino, Via Madonna delle Carceri, I-62032 Camerino (MC), Italy*
[2]*Istituto Nazionale di Fisica Nucleare (INFN), Laboratori Nazionali di Frascati, Via E. Fermi, 40, I-00044 Frascati (Roma), Italy*
(Received 12 November 2003; revised manuscript received 23 March 2004; published 6 July 2004)

Local structure of binary mixtures has been usually determined by diffraction techniques. In the past few years the analysis of x-ray absorption spectroscopy data has been proved to be a powerful tool for an accurate determination of the structure of solid and liquid systems, complementary to x-ray or neutron scattering methods. In this paper we report about a procedure to extract pair correlation functions of liquid and disordered binary mixtures from x-ray absorption fine structure (XAFS) data, satisfying both long-distance behavior and long wavelength limit of Bhatia-Thornton structure factors. An application to accurate XAFS data collected on a CuSn binary metal alloy (Cu6Sn5) is reported and compared with existing models.

DOI: 10.1103/PhysRevB.70.014101 PACS number(s): 61.10.Ht, 61.25.Mv

I. INTRODUCTION

Binary metal alloys are a wide class of materials, with a variety of structural and electronic properties determined by the different solubility of the individual components. While solid metal alloys are relevant to numerous technological applications (coils for hybrid magnets, electrodes, lifting contacts, dental materials), molten alloys are especially interesting from the point of view of basic physics. Indeed a detailed knowledge of their structural properties and in particular an accurate investigation of their short-range correlations could be essential to understand interactions between different chemical species under thermodynamic equilibrium conditions and for the development of interatomic potentials.

In spite of their interest, very few experimental studies have been devoted to reveal the type of short-range order in binary alloys. A typical question to be answered is whether these systems will phase separate (like atom nearest neighbors) or order (unlike atom nearest neighbors).

In a binary mixture, the set of three pair distribution functions $g_{\alpha\beta}(r)$ necessary for a complete description of two-body correlations has been usually determined by diffraction techniques (see Ref. 1 for a review). Neutron diffraction provides information on both short-range and long-range $g_{\alpha\beta}(r)$ properties, but its application is limited to systems for which a complete set of contrasting isotopes is available. Moreover, these experiments are expensive and time consuming hindering the performance of systematic studies on the evolution of structural properties as a function of thermodynamic variables (pressure and/or temperature) or concentration.

In the past decades the x-ray absorption spectroscopy (XAS) has been proved to be a powerful tool for an accurate determination of the structure of liquid and highly disordered materials[2] even under extreme high-pressure[3] and/or high temperature conditions (see Ref. 4 and references therein). Modulations of the absorption cross section above a deep core level excitation edge allow one to investigate the environment of the photoabsorber in a range limited by the photoelectron mean free path. One of the most appealing features of the XAS technique is the possibility to determine the atomic environment of a selected atomic species simply by tuning the energy of the incoming beam around its *K*-edge.

However determining pair distribution functions from a set of XAS data is a challenging problem especially for multicomponent systems. The current strategy for the structural refinement from XAS data requires modeling of the distributions as a superposition of distinct peaks whose parameters are fitted to the experimental spectrum. This strategy is adopted by the GNXAS multiple-scattering data-analysis method[5,6] and has been extended to include multiedge structural refinements[7] in multicomponent systems for an accurate determination of the local environment of the different atomic species.

In highly disordered systems, peaks overlap in a continuous broadened distribution showing usually a distinct first peak corresponding to closest-neighbors distance. While the application of a peak-fitting strategy, limited to the first peak is still reasonable, it has been shown that a strong correlation between coordination numbers and shape parameters of the model distribution can lead to misleading results if the fit is performed without constraints.[4,8]

A simple but rigorous method overcoming this limitation using physical constraints into a still model dependent peak-fitting approach has been introduced for monoatomic systems[8] and extended to ionic binary liquids.[9]

The purpose of this paper is to report a new scheme to refine partial distribution functions, starting from a set of realistic pair distributions provided by computer simulations or diffraction experiments, which fully generalize this successful approach to liquid and disordered binary systems. This method allows us to refine the short-range peaks of a set of model partial distribution functions with constraints derived from long-range properties of the mixture, as the long-wavelength limits of Bhatia-Thornton structure factors.[10] This approach is not limited to melts of metal alloys, but it can be applied to all binary liquids and possibly extended to their disordered solid phases (amorphous, glasses, etc.) for which experiments are feasible, but a valid data-analysis method is still missing.

Here, the method is applied to determine the local structure of a liquid Cu6Sn5 alloy, for which accurate XAS spec-

tra have been measured and valid starting models can be found in the literature.[11,12]

The paper is organized as follows. In Secs. II A–II B, the background to the analysis of XAS spectra of liquids is reported. In Sec. II C, the scheme for the analysis of binary mixtures is described in detail. Its implementation in the framework of GNXAS is discussed in Sec. II D. In Sec. III, the application to a liquid Cu6Sn5 alloy at 1073 K is reported and results regarding its local structure compared with that of component metals are discussed. Section IV is devoted to concluding remarks.

II. METHOD: XAS REFINEMENT OF MOLTEN BINARY MIXTURES

A. Background

In a multicomponent system, XAS oscillations above the edge of a given photoabsorbing atom contain information on the pair distribution functions associated with all of the atoms surrounding the photoabsorber. If $\gamma^{(2)}_{\alpha\beta}(k,r)$ is the XAS signal corresponding to a single atom pair[5] at distance r, the total pair signal $\langle\chi_\alpha(k)\rangle$ associated with the XAS core level spectrum of the atom species α is given by an integral involving the corresponding distribution functions[13]

$$\langle\chi_\alpha(k)\rangle = \sum_\beta \int_0^\infty 4\pi\rho_\beta r^2 g_{\alpha\beta}(r)\gamma^{(2)}_{\alpha\beta}(k,r)dr, \qquad (1)$$

where $k=\sqrt{2m(E-E_0)}/\hbar$ is the modulus of the photoelectron wave vector (E_0 is the threshold energy).

The extraction of pair correlation functions from a set of XAS data is a rather complicated problem, as a simple Fourier transform gives a radial function containing phase and amplitude modulations which does not correspond to a real $g(r)$ distribution even in the simplest case of monoatomic systems. The current "peak-fitting" strategy for the structural refinement of XAS data consists in modeling the distributions as a superposition of successive peaks associated with the neighboring atomic shells, depending on structural parameters which are optimized to the experimental spectra.[6] Non-Gaussian model distributions have been introduced to account for the increased disorder.[13,14] This approach requires that each of the radial distribution functions is composed of isolated peaks and it is clearly appropriate for molecules or crystals. An advanced method, denominated GNXAS, for computing the XAS $\gamma^{(n)}_{\alpha\beta}(k,r)$ n-body signals and their averages [see Eq. (1) for two-body terms] has been developed and applied extensively in the last decade. Details about the computational techniques and structural refinements can be found in the reference GNXAS papers.[5,6]

A development relevant to the present study has been the extension of the GNXAS data-analysis method to combined multiedge refinements[7] which opened the way to a robust structural XAS data-analysis in multicomponent systems. In practice, the refinement process can include all of the XAS signals **(**$\langle\chi_\alpha(k)\rangle$**)** measured for each atomic species and core levels of a given sample using the corresponding distribution functions $[g_{\alpha\beta}(r)]$. In a binary mixture or compound AB, the three partial pair distribution functions $g_{AA}(r)$, $g_{BB}(r)$, and $g_{AB}(r)$, are associated with two independent set of measurements $\langle\chi_A(k)\rangle$ and $\langle\chi_B(k)\rangle$ involving the two different chemical species. Moreover, different core levels of the same atom can be measured and analyzed simultaneously.[7]

In highly disordered systems, like amorphous or liquid substances, peaks are merged in a broadened distribution with a well-defined closest approach distance and asymptotic $r\to\infty$ limit $g_{\alpha\beta}(r)=1$. The application of the peak-fitting approach seems still reasonable, as the short-range nature of the technique makes the total signal dominated by the contribution corresponding to the first peak of the distribution. However it has been proved[4,8] that strong correlations between coordination number and shape parameters can easily lead to unphysical results, such as unacceptably low coordination numbers and narrow widths of the first peak.

A successful approach to tackle this problem is to introduce suitable physical constraints accounting for the long-range properties of the disordered system, to which XAS is not sensitive. A rigorous method to introduce physical constraints into a still model dependent peak-fitting approach has been introduced for a single component system[8] and extensively applied in the past few years. The essential steps of the method are reported below.

B. Constraints for the short-range structure of monoatomic liquids

The refinement procedure proposed in Ref. 8 starts from a realistic model $g(r)$, provided by complementary techniques, which is supposed to have the correct long-distance behavior $\lim_{r\to\infty} g(r)=1$ and the proper compressibility limit

$$\lim_{q\to 0} S(q) = \lim_{q\to 0}\left[1 + 4\pi\rho\int_0^\infty r^2[g(r)-1]\frac{\sin(qr)}{qr}dr\right] = \frac{\rho K_T}{\beta}, \qquad (2)$$

where K_T is the isothermal compressibility and $\beta\equiv(k_BT)^{-1}$. Here q is the scattering wavevector modulus $q=4\pi/\lambda\,\sin(\theta/2)$.

The $g(r)$ can be generally decomposed into a short-range peak plus a long-range tail which is kept fixed during the refinement as it involves distances to which x-ray absorption fine structure (XAFS) is not sensitive. Floating parameters defining the short-range peaks are constrained in order to maintain the compressibility limit (2) while $g(r)$ [and the corresponding $S(q)$] is changed to achieve the better agreement with the experimental signal. Expanding the variation $\Delta S(q)$ [corresponding to a change $\Delta g(r)$ in the pair distribution function] in a Taylor series about $q=0$, one obtains the following set of constraints:

$$\left(\left.\frac{\partial^{2m}\Delta S(q)}{(\partial q)^{2m}}\right|_{q=0}\right) = 0 \Leftrightarrow 4\pi\rho\int_0^\infty r^{2+2m}\Delta g(r)dr = 0. \qquad (3)$$

A practical and efficient way to implement these constraints in the framework of the GNXAS approach is to decompose the initial $g(r)$ model into one or two short-range peaks plus a long range tail

$$4\pi\rho r^2 g(r) = N_1 p_1(r|R_1,\sigma_1^2,\beta_1) + N_2 p_2(r|R_2,\sigma_2^2,\beta_2) + 4\pi\rho r^2 g_t(r), \quad (4)$$

where $p_j(r|R_j,\sigma_j^2,\beta_j)$ is a normalized Γ-like distribution function.[14,15] The sum of these three contributions will give the total two-body XAFS signal.

During an actual XAFS structural refinement the tail contribution $g_t(r)$ is kept fixed. The refinement of the short-range peaks is performed with constraints, resulting from Eq. (3) for $m=0$ and $m=1$.

$$N_1 + N_2 = N^{\text{tot}}$$

$$N_1(R_1^2+\sigma_1^2) + N_2(R_2^2+\sigma_2^2) = M_2^{\text{tot}}, \quad (5)$$

where N^{tot} and M_2^{tot} are the total coordination number and the total second moment of the matter distribution about $r=0$ associated with the two short-range peaks.

C. Extension of the method to molten binary mixtures

As far as the structure of a binary mixture is concerned, a set of three partial pair distribution functions describing correlations between each couple of atomic species is required. The methodology introduced for monoatomic liquids cannot be applied to the refinement of the three-partial distributions as the long-wavelength limit (2) is not valid for each of the $S_{\alpha\beta}(q)$ separately. The isothermal compressibility K_T is related to the long wavelength limits of partial structure factors $S_{\alpha\beta}(q)$ by the following equation:[16]

$$\lim_{q\to 0} \frac{S_{11}(q)S_{22}(q) - S_{12}^2(q)}{S_{cc}(q)/[c_2(1-c_2)]} = \rho k_B T K_T. \quad (6)$$

Since this relation involves the three $S_{\alpha\beta}(q)$ simultaneously, it is not useful to obtain constraints on the partial pair distribution functions. This is the mathematical consequence of the fact that partial distributions are all embedded in determining long-range properties of the alloy, and each of the $g_{\alpha\beta}(r)$ cannot be refined independently from the others. A particular case is represented by two-component charged liquids, as for example molten salts. In that case, Eq. (6) still holds, but requiring full screening in the Coulomb field, it simplifies to[17]

$$\lim_{q\to 0}[Z_1 S_{11}(q) = \sqrt{Z_1 Z_2} S_{12}(q) = Z_2 S_{22}(q)] = \rho k_B T K_T. \quad (7)$$

It follows from these limits that each partial $g_{\alpha\beta}(r)$ can be refined independently from the others extending the constraints originally derived for mono-atomic systems. The validity of this approach has been tested in a wide class of ionic[13] and super-ionic[9] binary salts.

For the general case of binary alloys we propose a refinement strategy. Thermodynamical properties of binary mixtures are directly related to a set of three structure factors $S_{NN}(q)$, $S_{cc}(q)$, and $S_{Nc}(q)$ introduced by Bhatia and Thornton.[10] These functions describe correlations between fluctuations in the total number of particles N, between fluctuations in concentration c and cross-correlations between N and c irrespective of the atomic species. Complete correspondence between Bhatia-Thornton and Faber-Ziman formalisms can be established comparing total scattering amplitudes from a binary mixture expressed in term of each of the structure factors sets. It results that $S_{cc}(q)$, $S_{NN}(q)$, and $S_{Nc}(q)$ are related to the $S_{11}(q)$, $S_{22}(q)$, and $S_{12}(q)$ by the following equations:

$$S_{NN}(q) = c_1 S_{11}(q) + c_2 S_{22}(q) + 2(c_1c_2)^{1/2} S_{12}(q),$$

$$S_{cc}(q) = c_1 c_2 [c_2 S_{11}(q) + c_1 S_{22}(q) - 2(c_1c_2)^{1/2} S_{12}(q)],$$

$$S_{Nc}(q) = c_1 c_2 \left[S_{11}(q) - S_{22}(q) + \frac{c_2 - c_1}{(c_1c_2)^{1/2}} S_{12}(q) \right]. \quad (8)$$

The long-wavelength limits of the Bhatia-Thornton structure factors have a simple physical meaning[10] representing mean-square fluctuations in the number of particles $\langle(\Delta N)^2\rangle$, in the concentration $\langle(\Delta c)^2\rangle$ and in the correlation between the two fluctuations Δc and $\Delta N = \Delta N_1 + N_2$

$$S_{NN}(0) = \langle(\Delta N)^2\rangle/N = (N/V)k_B T K_T + \delta^2 S_{cc}(0),$$

$$S_{cc}(0) = N\langle(\Delta c)^2\rangle = N k_B T \Big/ \left(\frac{\partial^2 G}{\partial c^2}\right)_{T,p,N},$$

$$S_{Nc}(0) = \langle \Delta N \Delta c\rangle = -\delta S_{cc}(0), \quad (9)$$

where K_T is the isothermal compressibility, G is the Gibbs free energy, P is the pressure, and δ is a dilatation factor $\delta = (v_1 - v_2)/[c_1 v_1 + (1-c_1)v_2] = N/V(v_1 - v_2)$ where v_1 and v_2 are the partial molar volumes per atom of the two species defined by $v_\alpha = (\partial V/\partial N_\alpha)_{T,p,N_\beta}$, $\alpha,\beta = 1,2$. Explicit forms for the $S_{cc}(0)$ have been derived by Bhatia and Thornton[10] for different types of solutions.

Physical constraints on the partial pair distribution functions, can be derived from the three long-wavelength limits of Bhatia-Thornton structure factors reported in Eqs. (9). Since the corresponding $g_{NN}(r)$, $g_{Nc}(r)$, and $g_{cc}(r)$ distributions are linear combinations of the $g_{11}(r)$, $g_{22}(r)$, and $g_{12}(r)$ functions, we can obtain from Eq. (9) a set of constraints on linear combinations of these three distributions. The XAS refinement of $g_{\alpha\beta}(r)$ will modify only the shape of their short-range peaks, while maintaining unchanged the long-range limit of the $g_{\alpha\beta}(r)$ and of the corresponding Bhatia-Thornton structure factors. The fundamental hypothesis of our construction is that the right-hand side of Eqs. (9) is not affected by a change in the short-range side of the partial pair distribution functions similarly to the monoatomic case.[8] Parameters defining the short-range peaks of the partial distribution functions can be then refined using the experimental spectra, providing that differences in the structure factors $S_{NN}(q)$, $S_{Nc}(q)$, and $S_{cc}(q)$ induced by changes of the pair distribution functions do not alter their $q=0$ limit:

$$\lim_{q\to 0}\Delta S_{NN}(q) = \lim_{q\to 0} 4\pi\rho \int_0^\infty dr r^2 \frac{\sin qr}{qr} \{c_1^2 \Delta g_{11}(r) + c_2^2 \Delta g_{22}(r) + 2c_1c_2 \Delta g_{12}(r)\} = 0,$$

$$\lim_{q\to 0}\Delta S_{cc}(q) = \lim_{q\to 0} 4\pi\rho c_1^2 c_2^2 \int_0^\infty dr r^2 \frac{\sin qr}{qr}\{\Delta g_{11}(r) + \Delta g_{22}(r) - 2\Delta g_{12}(r)\} = 0,$$

$$\lim_{q\to 0}\Delta S_{Nc}(q) = \lim_{q\to 0} 4\pi\rho c_1 c_2 \int_0^\infty dr r^2 \frac{\sin qr}{qr}\{c_1\Delta g_{11}(r) - c_2\Delta g_{22}(r) + (c_2 - c_1)\Delta g_{12}(r)\} = 0. \quad (10)$$

These conditions of invariance of the Bhatia-Thornton structure factors near $q=0$, can be exploited to obtain useful physical constraints for the structural parameters defining the short-range structure, following the same strategy adopted for the monoatomic case,[8] as illustrated in the next section.

D. Constraints for the short-range structure of binary mixtures

Let us suppose that each initial model $g_{\alpha\beta}(r)$ can be decomposed into two short-range peaks plus a long-range tail. Any functional form allowing to reproduce the shape of the first peaks of the distributions, depending on a limited number of parameters and with defined even order momenta about $r=0$ can be arbitrarily chosen. A suitable model function, able to account for asymmetric bondlength distributions, is the so-called Γ-like function[14,15] depending only on three parameters R, σ^2, and β representing average, variance, and skewness of the distribution. This function has been proved to be an efficient choice for modeling pair distribution in both solids[13] and liquids[14] but the method applies to any other functional model able to account for deviations from the Gaussian distribution or the Gaussian model itself.

Constraints on parameters defining the short-range peaks can be easily deduced from Eq. (10), writing a Taylor expansion of $\Delta S_{NN}(q)$, $\Delta S_{cc}(q)$, and $\Delta S_{Nc}(q)$ about $q=0$ as shown in Sec. II B. Modeling short-range peaks as Γ-like functions, the set of model distributions can be written as follows:

$$4\pi\rho_1 r^2 g_{11}(r) = \sum_{j=I}^{II} N_{11}^j p_{11}^j(r|R_{11}^j, {\sigma_{11}^j}^2, \beta_{11}^j) + 4\pi\rho_1 r^2 g_{11}^t(r),$$

$$4\pi\rho_2 r^2 g_{22}(r) = \sum_{j=I}^{II} N_{22}^j p_{22}^j(r|R_{22}^j, {\sigma_{22}^j}^2, \beta_{22}^j) + 4\pi\rho_2 r^2 g_{22}^t(r),$$

$$4\pi\rho_2 r^2 g_{12}(r) = \sum_{j=I}^{II} N_{12}^j p_{12}^j(r|R_{12}^j, {\sigma_{12}^j}^2, \beta_{12}^j) + 4\pi\rho_2 r^2 g_{12}^t(r), \quad (11)$$

where $p_{\alpha\beta}^j(r|R_{\alpha\beta}^j, \sigma_{\alpha\beta}^j, \beta_{\alpha\beta}^j)$ are normalized Γ-like functions depending on three shape parameters. In Eq. (11) each partial pair distribution $g_{\alpha\beta}(r)$ has been decomposed into a sum of two Γ-like functions $p_{\alpha\beta}^I$, $p_{\alpha\beta}^{II}$, and a long-range tail $g_{\alpha\beta}^t(r)$ which is kept fixed during the XAS refinement process.

Writing this decomposition in Eq. (10) we obtain the following system of constraining equations, corresponding to terms with $m=0$ and $m=1$ in the Taylor expansion of $\Delta S_{NN}(q)$, $\Delta S_{cc}(q)$, and $\Delta S_{Nc}(q)$ about $q=0$:

$$\sum_{j=I}^{II}[c_1 N_{11}^j + c_2 N_{22}^j + 2c_1 N_{12}^j] = M_0^A,$$

$$\sum_{j=I}^{II}[c_1 c_2^2 N_{11}^j + c_1^2 c_2 N_{22}^j - 2c_1^2 c_2 N_{12}^j] = M_0^B,$$

$$\sum_{j=I}^{II}[c_1 c_2 N_{11}^j - c_1 c_2 N_{22}^j - c_1(c_2 - c_1) N_{12}^j] = M_0^C,$$

$$\sum_{j=I}^{II}[c_1 N_{11}^j({R_{11}^j}^2 + {\sigma_{11}^j}^2) + c_2 N_{22}^j({R_{22}^j}^2 + {\sigma_{22}^j}^2) + 2c_1 N_{12}^j({R_{12}^j}^2 + {\sigma_{12}^j}^2)] = M_2^A,$$

$$\sum_{j=I}^{II}[c_1 c_2^2 N_{11}^j({R_{11}^j}^2 + {\sigma_{11}^j}^2) + c_1^2 c_2 N_{22}^j({R_{22}^j}^2 + {\sigma_{22}^j}^2) - 2c_1^2 c_2 N_{12}^j({R_{12}^j}^2 + {\sigma_{12}^j}^2)] = M_2^B,$$

$$\sum_{j=I}^{II}[c_1 c_2 N_{11}^j({R_{11}^j}^2 + {\sigma_{11}^j}^2) - c_1 c_2 N_{22}^j({R_{22}^j}^2 + {\sigma_{22}^j}^2) - c_1(c_2 - c_1) N_{12}^j({R_{12}^j}^2 + {\sigma_{12}^j}^2)] = M_2^C, \quad (12)$$

where M_0^A, M_0^B, M_0^C, M_2^A, M_2^B, and M_2^C are linear combinations of zero- and second-order momenta of the functional forms modeling the short-range peaks of the pair distribution functions. These quantities are calculated for the model distributions and then kept fixed during all the XAS refinement procedure, as they maintain the long-range behavior of the distribution. At each step of the minimization, structural parameters $R_{\alpha\beta}^j$, ${\sigma_{\alpha\beta}^j}^2$, and $\beta_{\alpha\beta}^j$ are floated in order to minimize a residual function, and the system (12) is solved calculating coordination numbers $N_{\alpha\beta}^j$ which satisfy the correct long-range limits for the pair distribution functions.

III. APPLICATION: THE SHORT-RANGE STRUCTURE OF MOLTEN Cu6Sn5

The constrained-refinement procedure described in the previous section has been applied to a molten Cu6Sn5 alloy at 1073 K. In this section, we report this analysis showing the main features of the approach and its capability of giving reliable results on the structural refinement of liquid binary mixtures. Thermodynamical and structural properties of liquid Cu-Sn alloys have been extensively investigated.[10,18] The partial structure factors of molten Cu6Sn5 have been determined by isotopic substitution neutron diffraction.[12] In Ref. 11, partial structure factors $S_{\alpha\beta}(q)$ and corresponding distribution functions were derived by x-ray scattering. Partial interference functions were obtained from the total intensity scattered by alloys of different concentrations assuming the partial structure factors to be concentration independent. It must be stressed that this hypothesis excludes any possibility of investigating the changes in the composition of local structure as a function of concentration.

A. Experimental details

Cu6Sn5 alloys were produced mixing high purity CuO and SnO oxides powders, in the appropriate weight ratios to obtain the proper 0.545 at. %-Cu concentration. The mixture was finely ground, mixed with inert graphite powder (1:10 weight ratio), and then pressed into pellets (thickness $\approx$1 mm). Pellets were heated in high-vacuum up to 1400 K. Copper and tin oxides decompose around 900 K forming metallic particles which alloy completely in the phase diagram region above the liquidus curve. X-ray diffraction measurements showed that the final samples were a dispersion of alloy particles, with a narrow spreading around the average concentration. High temperature measurements were performed using a high vacuum special furnace (L'Aquila-Camerino oven[19]) designed to collect XAS spectra and x-ray diffraction (XRD) patterns at high temperatures. XAS spectra were collected at Cu and Sn *K*-edges at the ESRF-BM29[20] and LURE-D42 beamlines. The availability of spectra at both edges allows a simultaneous double-edge refinement of the pair distribution functions.

B. Data analysis and results

The structural refinement was performed assuming the set of $g_{\mathrm{CuSn}}(r)$, $g_{\mathrm{CuCu}}(r)$, and $g_{\mathrm{SnSn}}(r)$ measured by XRD (Ref. 11) as a starting model. We note that, as $q \rightarrow 0$, the set of partial structure factors measured by XRD extrapolates to zero in disagreement with the thermodynamic results.[18] However XAFS is only sensitive to short-range ordering and therefore we cannot provide a new measurement of $S_{\alpha\beta}(0)$ from XAFS data, but just constrain the refinement to keep constant the long-wavelength limit of a given model (provided by XRD in the present case), which is assumed to be correct in describing medium and long distances.

As a first step of data analysis, the compatibility between the experimental signal and the starting model has been verified. For this purpose, two-body $\gamma^{(2)}(k)$ signals were calculated using the multiple-scattering code GNXAS[5–7] and averaged over the set of XRD-$g(r)$'s through Eq. (1). The comparison is reported in Fig. 1. The top and bottom panels refer, respectively, to Cu and Sn *K*-edge XAS signals. It is evident that signals associated with the model (solid lines) roughly reproduce the main features of the experimental signals (dots). However, phase and amplitude differences indicate that the shape of the first peaks can be refined exploiting the sensitivity of XAS to short-range details and its complementarity with scattering techniques.

For the purpose of the structural refinement, model distribution functions were decomposed according to the procedure reported in Sec. II D. The adopted decomposition is shown in Fig. 2. Each partial distribution function has been decomposed in a superposition of two Γ-like peaks plus a long-range tail, as indicated in Eq. (11). The Sn-Sn distribution function $g_{\mathrm{SnSn}}(r)$ can be reproduced using two Γ-like peaks while Cu-Cu and Cu-Sn distributions can be defined using a single dominant Γ-like peak. The structural refinement was performed as described in Sec. II D, floating the structural parameters associated with the peaks of the decomposition, throughout the minimization procedure. Data-analysis has been carried out within the GNXAS method, which is based on a minimization of a χ^2-like residual function in the space of structural and background parameters. Standard procedures suitable for nonlinear fitting problems are used to obtain best-fit estimates for structural parameters.

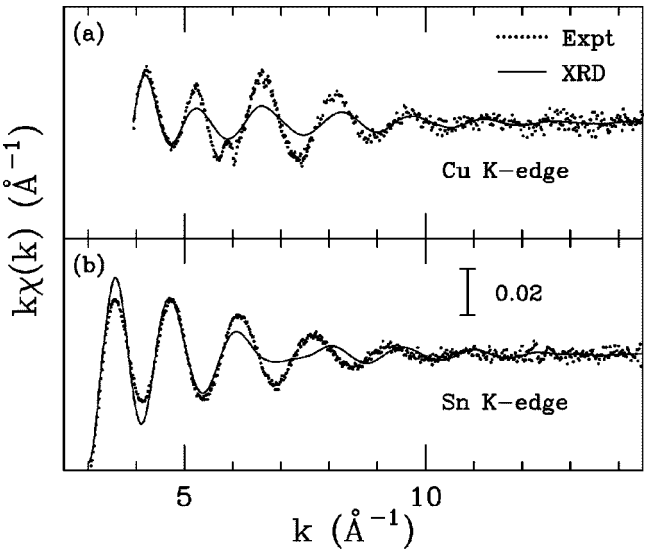

FIG. 1. Comparison between XAS $k\gamma^{(2)}(k)$ signals calculated from the partial distribution functions provided by XRD (Ref. 11) (solid line), and experimental signals (dots) measured on Cu6Sn5 at 1073 K. The top and bottom panels refer to Cu and Sn-edge XAS signals, respectively.

The physical constraints derived in Sec. II D have been implemented in the fitting routine (fitheo) of the GNXAS

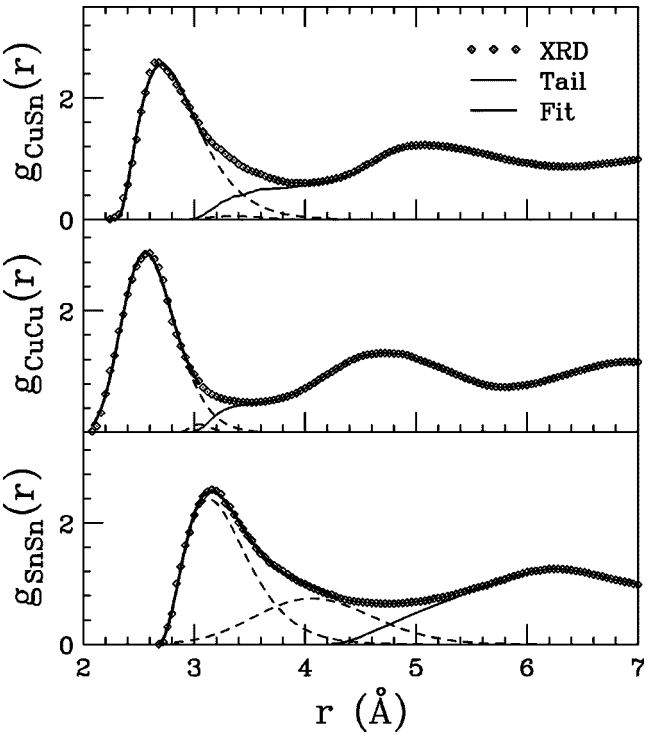

FIG. 2. Decomposition of the XRD (Ref. 11) distribution functions (diamonds) in two short-range Γ-like peaks (dashed lines) and a long-range tail (thin solid line).

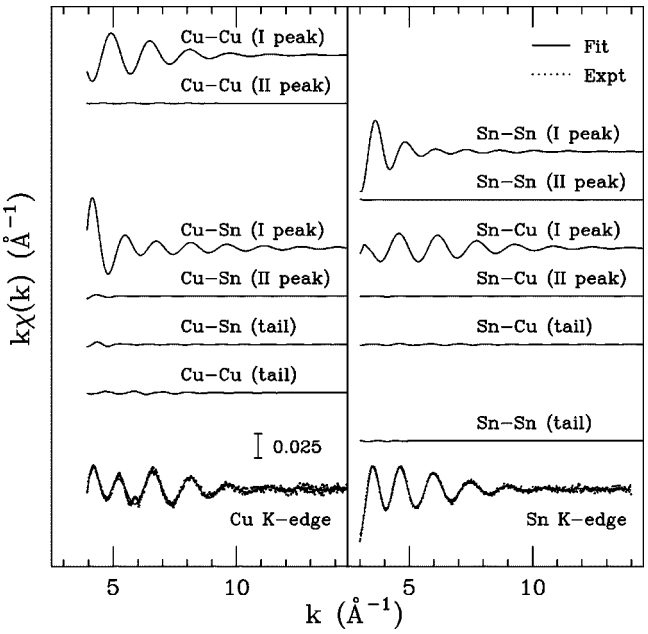

FIG. 3. Cu (left panel) and Sn (right panel) *K*-edge XAS experimental signals (Expt) of Cu6Sn5 at 1073 K, compared with the best-fit signal (Fit) obtained from the refinement of $g_{\mathrm{CuSn}}(r)$, $g_{\mathrm{CuCu}}(r)$, and $g_{\mathrm{SnSn}}(r)$ first peaks. The upper curves are the contributions associated with the individual two-body terms of the decomposition. The agreement is very good.

suite of programs. In particular, the linear combinations M_0^A, M_0^B, M_0^C, M_2^A, M_2^B and M_2^C, as well as concentration $c_1 = 0.545$ (and $c_2 = 1 - c_1$) [see Eq. (12)] have been kept fixed to the value calculated for the model distributions during all the refinement procedures. At each step of the minimization, structural parameters defining peaks of the decomposition are floated in order to minimize the difference between the simulation and experimental data and the system (12) is solved to obtain coordination numbers $N_{\alpha\beta}^j$ which satisfy the correct long-range limits for the $g(r)$'s. Parameters associated with the second peaks of the $g_{\mathrm{CuSn}}(r)$, $g_{\mathrm{CuCu}}(r)$, and $g_{\mathrm{SnSn}}(r)$ distributions were kept fixed as the corresponding signals give a negligible contribution to the total XAS signals. Also the tail contribution was kept fixed, as it involves distances to which XAS is not sensitive. In this way, the floating structural parameters are only 9. In Fig. 3 our best-fit results are reported. The upper curves in each panel are the $k\gamma^{(2)}(k)$ signals corresponding to the individual two-body terms of the decomposition. Clearly, the dominant contributions are those associated with the first peaks of each of the $g(r)$'s. The main frequency and amplitude of the experimental signal (Expt) are accurately reproduced. There is a slight mismatch between experimental and two-body calculated signals observed especially at the Cu K-edge around 6 Å^{-1}, that corresponds to a very weak high-frequency contribution at both edges. This tiny residual oscillation can be tentatively assigned to a weak multiple-scattering collinear signal associated with Cu-Sn-Cu triplet configurations as we verified by direct comparison with three-body calculations. In any case, the quality of the two-body refinement indicates that the contribution of three-body signals in our data is practically negligible.

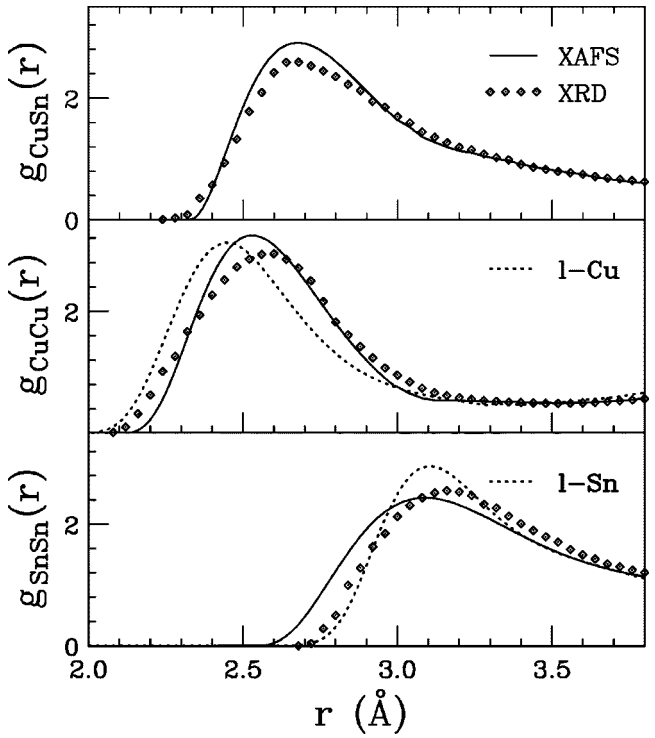

FIG. 4. Comparison between distribution functions as obtained by XAS data analysis (solid line) and previous XRD models[11] (diamonds). The $g(r)$'s of pure Cu and Sn measured by XAS (dotted) are also shown for comparison.

Parameters obtained from the best-fit were used to reconstruct the short-range side of $g_{\mathrm{CuSn}}(r)$, $g_{\mathrm{CuCu}}(r)$, and $g_{\mathrm{SnSn}}(r)$ distribution functions. Reconstructed partial distributions (solid line) are compared with the XRD starting model (diamonds) in Fig. 4. It is clear that the $g_{\mathrm{CuCu}}(r)$ and $g_{\mathrm{SnSn}}(r)$ distributions differ from the original model, especially on the short-distances side, to which XAS is exceptionally sensitive. The first maximum and the foot of the $g_{\mathrm{SnSn}}(r)$ distribution are shifted about 0.1 Å toward shorter distances, indicating that the Sn-Sn average bond length and the corresponding closest approach distance are affected by the presence of Cu atoms. Similarly, the rise of the $g_{\mathrm{CuCu}}(r)$ peak is steeper and shifted to longer distances while the most probable Cu-Cu bond length is slightly shorter with respect to the one measured by XRD. However, the first peak of the $g_{\mathrm{CuCu}}(r)$ distribution is clearly shifted toward longer distances with respect to that of pure liquid Cu as measured by XAS (dotted). A similar shift in the opposite direction is observed for the first $g_{\mathrm{SnSn}}(r)$ peak (lower panel) as compared with the XRD starting data and with that of pure Sn reconstructed by XAS at much lower temperature (510 K, dotted line). The $g_{\mathrm{CuSn}}(r)$ short-range distribution (upper panel of Fig. 4) is slightly higher but qualitatively similar to that found by XRD.

The $S_{\mathrm{CuSn}}(q)$, $S_{\mathrm{CuCu}}(q)$, and $S_{\mathrm{SnSn}}(q)$ calculated by Fourier back-transformation from the $g_{\mathrm{CuSn}}(r)$, $g_{\mathrm{CuCu}}(r)$, and $g_{\mathrm{SnSn}}(r)$ reconstructed by XAFS, have been compared also with the ND structure factors.[12] The curves are compatible within the noise level and the uncertainties associated with applying Fourier inversion.

Looking at these results, it is clear that the shape of the $g_{CuCu}(r)$ and $g_{SnSn}(r)$ is affected by the presence of unlike atoms and therefore the assumption of independence on atomic concentrations at the basis of previous XRD studies[11] is not confirmed. The effect on the first-neighbor distances of like atoms is of the order of 0.1 Å, quite important as compared with the difference in the average distances of the pure elements (about 0.6 Å). Clearly, the relative size of the Sn and Cu atoms and their different interatomic average distances play a role in determining the structural properties of the mixture. While the detailed explanation of this effect is beyond the scope of the present paper, it is important to remark that a deep structural insight about local atomic correlations can be obtained by application of the XAS data-analysis method presented here to accurate multiple-edge data of binary alloys. The combined use of XAS and XRD or ND data makes it possible to obtain a very accurate reconstruction of the details of the local structure of binary disordered alloys.

IV. CONCLUSIONS

The problem of a reliable determination of the local structure in binary mixtures using the x-ray absorption spectroscopy has been tackled taking into account the previous knowledge, mainly related to neutron and x-ray diffraction results, and several recent advances in the field. In particular, the use of multiple-edge XAS structural refinement is shown to be able to provide accurate structural information about the short-range partial distribution functions. However, in a disordered system such as a liquid alloy, it is essential to combine the long-range structural information obtained by diffraction techniques with the accurate short-range XAS sensitivity. In a monoatomic liquid, this results in a set of constraints for the shape of the first-neighbor peak of the distribution. In this paper, we have developed a constrained "peak-fitting" refinement of the three partial pair distribution functions defined for a binary liquid. The constraints on the structural parameters defining the first-neighbor peaks are obtained using the long wavelength limits of the Bhatia-Thornton structure factors. The use of the constraints strongly reduces the uncertainty in the shape of the reconstructed distribution functions, which are forced to satisfy the proper long-distance behavior and thermodynamic limits. This method is applied to reconstruct the local structure of the Cu6Sn5 binary alloy, for which pioneering neutron diffraction measurements with the isotope substitution technique and accurate x-ray diffraction data are available. The approach is shown to be successful in obtaining a very accurate simulation of the XAS data using previous diffraction results as a starting model. The Cu-Cu and Sn-Sn first-neighbor peaks of the partial distribution functions have been found to shift with respect to the original positions in the pure Cu and Sn melts. Average first-neighbor Sn-Sn distances are found to be shorter than in pure Sn, and a shift in the opposite direction is found for Cu-Cu pairs. The like-unlike Cu-Sn distribution is located at intermediate distances and is found in good agreement with previous works. These results indicate that the assumption of independence on atomic concentrations used in previous XRD studies is not fully justified. In fact, the shape of the $g_{CuCu}(r)$ and $g_{SnSn}(r)$ distributions is affected by the presence of unlike atoms with a clear shift of the first-peak of about 0.1 Å, quite remarkable as compared with the difference in the average distances in the pure liquids ($\sim$0.6 Å).

These results show that the x-ray absorption spectroscopy (XAS) is a powerful tool for an accurate determination of the structure of disordered binary alloys, complementary to x-ray and neutron scattering techniques. The method and application presented here are intended to provide a reference detailed study for future application on multicomponent disordered systems.

*Electronic address: angela.trapananti@unicam.it

[1] J. E. Enderby, Contemp. Phys. **24**, 561 (1983).
[2] E. D. Crozier, J. J. Rehr, and R. Ingalls, in *X-Ray Absorption: Principles, Applications, Techniques of EXAFS, SEXAFS, and XANES*, edited by D. C. Koningsberger and R. Prins (Wiley, New York, 1988), pp. 375–384.
[3] R. Ingalls, G. A. Garcia, and E. A. Stern, Phys. Rev. Lett. **40**, 334 (1978).
[4] A. Filipponi, J. Phys.: Condens. Matter **13**, R23 (2001).
[5] A. Filipponi, A. Di Cicco, and C. R. Natoli, Phys. Rev. B **52**, 15 122 (1995).
[6] A. Filipponi and A. Di Cicco, Phys. Rev. B **52**, 15 135 (1995).
[7] A. Di Cicco, Phys. Rev. B **53**, 6174 (1996).
[8] A. Filipponi, J. Phys.: Condens. Matter **6**, 8415 (1994).
[9] A. Di Cicco, M. Minicucci, and A. Filipponi, Phys. Rev. Lett. **78**, 460 (1997).
[10] A. B. Bhatia and D. E. Thornton, Phys. Rev. B **2**, 3004 (1970).
[11] D. M. North and C. N. J. Wagner, Phys. Chem. Liq. **2**, 87 (1970).
[12] J. E. Enderby, D. M. North, and P. A. Egelstaff, Philos. Mag. **14**, 961 (1966).
[13] A. Di Cicco, M. J. Rosolen, R. Marassi, R. Tossici, A. Filipponi, and J. Rybicki, J. Phys.: Condens. Matter **8**, 10 779 (1996).
[14] P. D' Angelo, A. D. Nola, A. Filipponi, N. V. Pavel, and D. Roccatano, J. Chem. Phys. **100**, 985 (1994).
[15] A. Filipponi and A. Di Cicco, Phys. Rev. B **51**, 12 322 (1995).
[16] J. G. Kirkwood and F. Buff, J. Chem. Phys. **19**, 774 (1951).
[17] N. H. March and M. P. Tosi, *Atomic Dynamics in Liquids* (Dover, New York, 1991).
[18] R. Turner, E. D. Crozier, and J. F. Cochran, J. Phys. C **6**, 3359 (1973).
[19] A. Filipponi and A. Di Cicco, Nucl. Instrum. Methods Phys. Res. B **93**, 302 (1994).
[20] A. Filipponi, M. Borowski, D. T. Bowron, S. Ansell, A. Di Cicco, S. De Panfilis, and J.-P. Itiè, Rev. Sci. Instrum. **71**, 2422 (2000).